EUROPEAN UROLOGY ONCOLOGY xxx (xxxx) xxx–xxx

available at www.sciencedirect.com
journal homepage: euoncology.europeanurology .com

European Association of Urology

Brief Report

FGFR1/3 Signaling as an Achilles' Heel of Phenotypic Diversity in Urothelial Carcinoma

Renate Pichler[a,†,*], *Nils C.H. van Creij*[b,†], *Laura S. Mertens*[c], *Francesco del Giudice*[d], *Florestan Koll*[e], *Francesco Soria*[f], *José Daniel Subiela*[g], *Henning Plage*[h], *Piotr Tymoszuk*[i], *Roman Mayr*[j], *Gerald Klinglmair*[a], *Andreas Seeber*[k,l], *Martin Pichler*[l,m,n], *Michael Günther*[o], *Steffen Ormanns*[o,p], *Eva Compérat*[q], *Roger Li*[r], *Marco Moschini*[s,t], *Benjamin Pradére*[u], *on behalf of the European Association of Urology-Young Academic Urologists Urothelial Carcinoma Working Group*

[a] *Department of Urology, Comprehensive Cancer Center Innsbruck, Medical University of Innsbruck, Innsbruck, Austria;* [b] *Division of Experimental Urology, Department of Urology, Medical University of Innsbruck, Innsbruck, Austria;* [c] *Department of Urology, Netherlands Cancer Institute, Amsterdam, The Netherlands;* [d] *Department of Maternal Infant and Urologic Sciences, Sapienza University of Rome, Policlinico Umberto I Hospital, Rome, Italy;* [e] *Department of Urology, Medical University of Graz, Graz, Austria;* [f] *Division of Urology, Department of Surgical Sciences, San Giovanni Battista Hospital, University of Studies of Torino, Turin, Italy;* [g] *Department of Urology, Instituto Ramón y Cajal de Investigación Sanitaria, Hospital Universitario Ramón y Cajal, Universidad de Alcalá, Madrid, Spain;* [h] *Department of Urology, Charité-Universitätsmedizin Berlin, Berlin, Germany;* [i] *Data Analysis Service Tirol, Wörgl, Austria;* [j] *Department of Urology, Caritas St. Josef Hospital, University of Regensburg, Regensburg, Germany;* [k] *Department of Hematology and Oncology, Comprehensive Cancer Center Innsbruck, Medical University of Innsbruck, Innsbruck, Austria;* [l] *Division of Oncology, Hematology and Palliative Care, General Clinics, Oberwart, Austria;* [m] *Division of Oncology, Department of Internal Medicine, Medical University of Graz, Graz, Austria;* [n] *Translational Oncology, II. Med Clinics University of Augsburg, Augsburg, Germany;* [o] *Innpath Institute of Pathology, Tirol Kliniken, Innsbruck, Austria;* [p] *Institute of Pathology, Neuropathology and Molecular Pathology, Medical University of Innsbruck, Innsbruck, Austria;* [q] *Clinical Institute of Pathology, Medical University of Vienna, Vienna, Austria;* [r] *Department of GU Oncology, H. Lee Moffitt Cancer Center and Research Institute, Tampa, FL, USA;* [s] *Department of Experimental Oncology/Unit of Urology, Urological Research Institute, IRCCS Ospedale San Raffaele, Milan, Italy;* [t] *Vita-Salute San Raffaele University, Milan, Italy;* [u] *Department of Urology UROSUD, La Croix Du Sud Hospital, Quint-Fonsegrives, France*

Article info

Article history:
Received 28 January 2025
Received in revised form 5 June 2025
Accepted July 14, 2025

Abstract

FGFR inhibitors are a new therapeutic option for urothelial carcinoma (UC) with *FGFR2/3* alterations. In this study, we analyzed genetic alterations, co-regulation, and differential expression for 45 genes encoding FGF, FGFR, or FGF-binding proteins (FGFBPs) in five published UC cohorts (n = 3939 MIBC) and 39 UC cell lines (DepMap portal). Network analyses identified *FGFR1/3* genes as critical oncogenic hubs, co-regulated with their ligands and co-receptors, and abundantly expressed at protein level in the HPA immunohistochemistry data set. Machine learning with 38 FGFR-, FGF-, and FGFBP-coding

† These authors contributed equally as first authors.
* Corresponding author. Department of Urology, Comprehensive Cancer Center Innsbruck, Medical University of Innsbruck, Anichstrasse 35, 6020 Innsbruck, Austria. Tel. +43 512 50424811; Fax: +43 512 50428365.
E-mail address: renate.pichler@i-med.ac.at (R. Pichler).

https://doi.org/10.1016/j.euo.2025.07.005

Please cite this article as: R. Pichler, Nils C.H. van Creij, L.S. Mertens et al., FGFR1/3 Signaling as an Achilles' Heel of Phenotypic Diversity in Urothelial Carcinoma, Eur Urol Oncol, https://doi.org/10.1016/j.euo.2025.07.005

Keywords:
FGFR signaling
FGFR inhibitors
Erdafitinib
Urothelial cancer
Consensus molecular classification

transcripts reproduced consensus molecular subtypes with high accuracy of 0.72–0.84 (Cohen's κ 0.59–0.77). *FGFR3* mutations in the transmembrane/hinge region, which were enriched in luminal papillary tumors, trigger ligand-independent signaling. Conversely, overexpression of *FGFR1* and its ligands and accessory protein transcripts indicates ligand-dependent FGFR1 signaling in stroma-rich and basal/squamous subtypes. The sensitivity of most DepMap UC cell lines to pan-FGFR inhibitors in the GDSC and PRISM drug screens was independent of *FGFR3* alterations. In vitro, erdafitinib reduced proliferation in *FGFR* wild-type UC cell lines in a similar manner to *FGFR3*-mutated cell lines. Our findings highlight FGFR1 and FGFR3 as pivotal signaling pathways with distinct, molecular subtype–specific activation mechanisms. The results suggest that FGFR inhibitors may have therapeutic applications beyond UC tumors with *FGFR2/3* alterations.

ADVANCING PRACTICE

What does this study add?
Erdafitinib is currently the only pan-FGFR inhibitor approved for metastatic urothelial cancer (UC) with *FGFR3* alterations following anti-PD-1 or anti-PD-L1 treatment. Our results for alteration rates, co-regulation patterns, and differential gene expression across consensus molecular UC subtypes for selected genes encoding FGFR, FGF, or FGF-binding proteins (FGFBPs) provide the first evidence that FGFR signaling is not only essential for luminal papillary (LumP) tumors characterized by frequent *FGFR3* mutations but also plays a significant role in other molecular subtypes, such as stroma-rich and basal/squamous (Ba/Sq) classes. We identified ligand-independent FGFR3 signaling in LumP tumors, and ligand- and FGFBP-dependent FGFR1 signaling in stroma-rich and Ba/Sq cancers. Resistance analysis revealed high sensitivity of UC cell lines to pan-FGFR inhibitors, irrespective of *FGFR3* mutation status. Erdafitinib reduced cell proliferation in five UC cell lines in a dose-dependent manner regardless of *FGFR3* alterations. The results suggest that FGFR inhibition may be effective in UC regardless of *FGFR* mutational status.

Clinical Relevance
This study highlights the essential role of FGFR1/3 signaling pathways in phenotypic variability in UC, extending beyond the LumP subtype to other molecular subtypes. Consequently, FGFR inhibitors may represent a promising therapeutic option for tumors without *FGFR2/3* alterations. Associate Editor: Dr. Jeremy Teoh.

Patient Summary
A drug called erdafitinib is approved for the treatment of urinary cancers with mutations in the *FGFR2* or *FGFR3* genes. Our study shows that FGFR3 and FGFR1 proteins also play a role in the development of urinary cancers with mutations in these genes. Patients with urinary cancer who do not have *FGFR2/FGFR3* mutations might also benefit from treatment with erdafitinib or other inhibitors of FGFR proteins.

Treatment of urothelial carcinoma (UC) is steadily shifting towards personalized medicine. FGFR inhibitors are now a promising therapy for UC with *FGFR2/3* genetic alterations. Erdafitinib is currently the only pan-FGFR inhibitor approved for metastatic UC with susceptible *FGFR3* alterations after previous anti-PD-1 or anti-PD-L1 treatment [1]. In non–muscle-invasive cancer (NMIBC), erdafitinib also shows efficacy in bacillus Calmette-Guérin–treated high-risk NMIBC with *FGFR2/3* alterations [2], and is being investigated in an intravesical delivery system (TAR-210) in MoonRISe-1, a phase 3 study comparing TAR-210 versus intravesical chemotherapy in patients with *FGFR2/3*-altered intermediate-risk NMIBC (NCT06319820).

Alternative approaches to patient selection for FGFR-targeted therapy beyond *FGFR* alteration status merit consideration. For instance, the phase 1b/2 FIERCE-22 study (NCT03123055) demonstrated comparable responses to vofatamab regardless of *FGFR3* alteration or wild-type (WT) status [3]. Response to therapy was more pronounced in luminal tumors but was also observed in other subtypes, including basal tumors [3]. In addition, an 80-gene RNA-based FGFR predictive response signature in high-risk NMIBC identified similar FGFR pathway activation not only in tumors with *FGFR* alterations but also in those with WT *FGFR*. This finding suggests potential for expanding the FGFR-targeted therapeutic landscape in UC [4].

Please cite this article as: R. Pichler, Nils C.H. van Creij, L.S. Mertens et al., FGFR1/3 Signaling as an Achilles' Heel of Phenotypic Diversity in Urothelial Carcinoma, Eur Urol Oncol, https://doi.org/10.1016/j.euo.2025.07.005

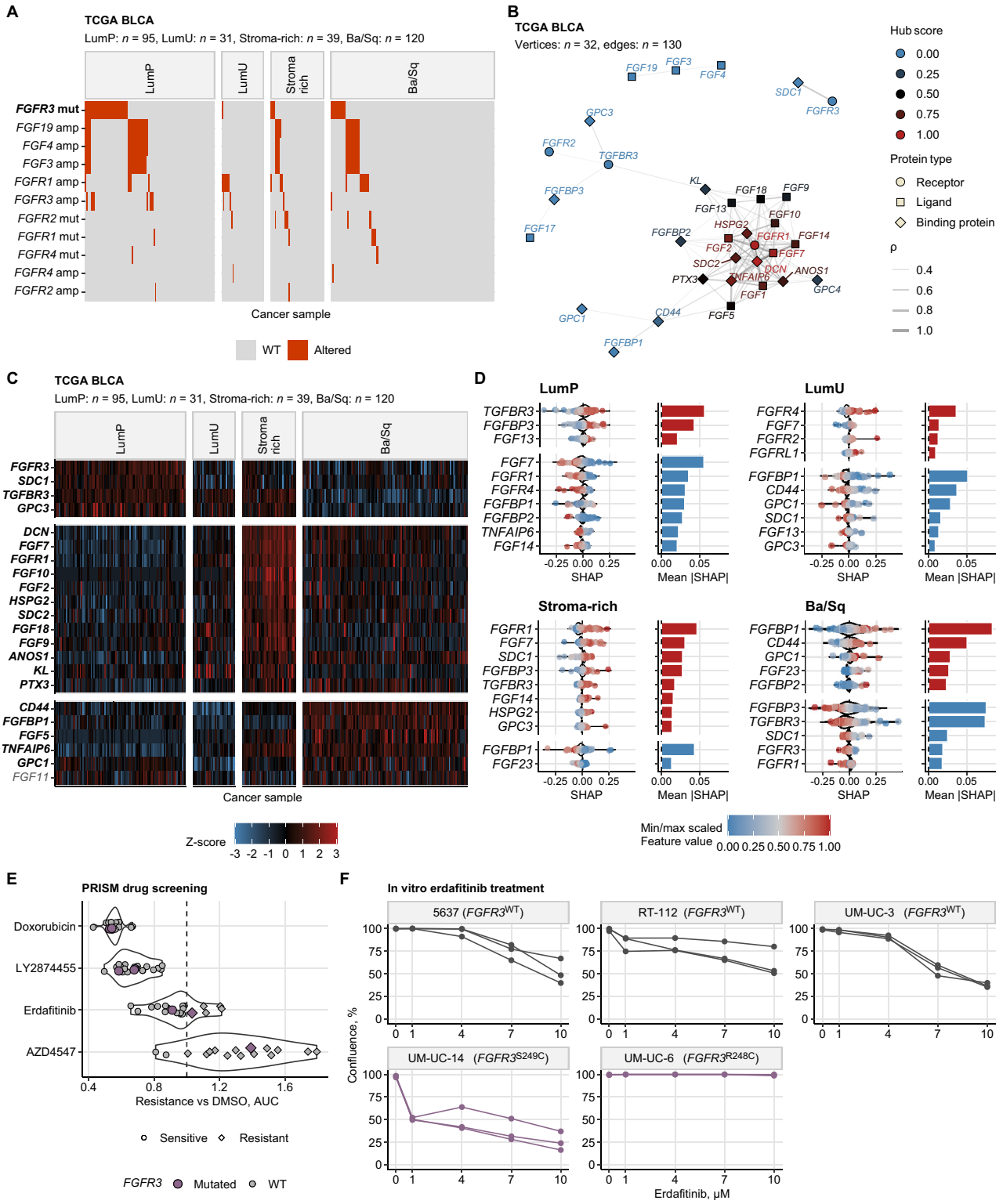

Please cite this article as: R. Pichler, Nils C.H. van Creij, L.S. Mertens et al., FGFR1/3 Signaling as an Achilles' Heel of Phenotypic Diversity in Urothelial Carcinoma, Eur Urol Oncol, https://doi.org/10.1016/j.euo.2025.07.005

The aim of our study was to characterize genetic alterations, co-regulation, and differential expression for 45 selected genes encoding FGF, FGFR, or FGF-binding protein (FGFBPs) across five published UC cohorts (GENIE BLCA [5], MSK IMPACT [6], TCGA [7,8], IMvigor [9], and BCAN [10]) including 3939 MIBC molecular profiles reflecting the complex network between FGFRs and their ligands and binding proteins.

Coexpression of FGFR-, FGF-, and FGFBP-coding genes was explored via network analyses. In addition, the response of 39 UC cell lines to pan-FGFR inhibitors was assessed in GDSC1/2 and PRISM drug screens available via the DepMap portal. *FGFR* wild-type and *FGFR3*-mutated UC cell lines were treated with 0, 1, 4, 7 or 10 μM erdafitinib (corresponding to 0–4.5 mg/l) in vitro. Prediction of drug resistance metrics (drug concentration required for 50% inhibition [IC_{50}] and area under the dose-response curve [AUC]) for the bulk cancers (TCGA GENIE BLCA, IMvigor, and BCAN) was performed with RIDGE linear models trained with drug response and transcriptome data for epithelial pan-cancer cell lines in the GDSC, CTRP2, and PRISM in vitro drug screening experiments. Machine learning (ML) was used to reproduce the consensus molecular subsets [11]. Human Protein Atlas immunohistochemistry data were used for validation of gene expression at the protein level. Detailed information on bioinformatics, characteristics of the collective cohorts, and the selected genes are presented in the Supplementary material and Supplementary Tables 1–3.

Somatic mutations of *FGFR3* (12–23% of cancers) and amplification of the 11q13 chromosome region in *FGF3/FGF4/FGF19* genes (6.3–11%) were the most common genetic alterations. *FGFR3* mutations were significantly enriched in luminal papillary (LumP) cancers (29–56%). *FGF3/FGF4/FGF19* gene amplifications were found in LumP (19%), stroma-rich (10%), and basal/squamous-like (Ba/Sq) cancers (8.3%), as shown in Fig. 1A, Supplementary Fig. 1, and Supplementary Tables 4 and 5). Most *FGFR1/2/3/4* mutations were classified as missense single-nucleotide polymorphisms. In the FGFR3 protein, mutations were located predominantly between ligand-binding IgG domains 2 and 3, with R248C and S249C hot spots (1.3–16%), and in the membrane-spanning hinge between the ligand-binding and kinase domains, with G370C, G372C, and Y373C hot spots (1.3–3.6%; Supplementary Figs. 2 and 3). These specific *FGFR3* mutations are implicated in constitutive, ligand-independent signaling [12].

At the mRNA level, *FGFR3*, *TGFBR3*, *FGFR1*, and *FGFR2* were the genes with the strongest expression. *FGF7*, *FGF2*, and *FGF11* were the most abundant ligand transcripts, while *SDC1*, *HSPG2*, and *CD44* had the highest mRNA counts among FGFBP-coding genes in UC tissue. *FGFR1*, *FGFR2,* and *FGFR3* receptors, as well as *SDC1*, *HSPG2*, *CD44*, *SDC4*, *GPC1* and *FIBP* binding protein transcripts, were also expressed in the DepMap UC cell lines. On immunohistochemistry, FGFR1/3/4 and FGFRL1 were the most abundant receptors, FGF7, FGF10, FGF3, FGF19, and FGF17 were the ligand proteins with the strongest expression, and SDC2, SDC1, GPC4, CD44, and SDC4 were the most abundant FGFBPs (Supplementary Figs. 4–7 and Supplementary Table 6).

Network analysis revealed a high degree of co-regulation of ligand, receptor, and FGFBP genes in UC tissue. This was particularly evident for *FGFR1* and genes encoding its ligands (*FGF2*, *FGF7*, *FGF10*) and co-receptors (*SDC2*, *DCN, HSPG2*). Importantly, *FGFR1* (hub score 0.91–1, degree 18), *FGF2* (hub score 0.85–0.96, degree 17–18), *FGF7* (hub score 0.94–0.97, degree 15–17), and *FGF10* (hub score 0.67–0.88, degree 14–17) were identified as highly connected hubs of the co-expression network (Fig. 1B and Supplementary

Fig. 1 – (A) Alterations in genes encoding FGFR, FGF, or FGFBP in consensus molecular classes of muscle-invasive bladder cancer (MIBC). Differences in the frequency of somatic mutations and copy-number variants in genes encoding FGFR/FGF/FGFBP between the luminal papillary (LumP), luminal unstable (LumU), stroma-rich, and basal/squamous-like (Ba/Sq) consensus molecular classes of MIBC in the TCGA cohort were assessed using a permutation text corrected for the false discovery rate (FDR). The presence or absence of selected genetic alterations (mut = mutation; amp = amplification; del = deletion) in the TCGA BLCA cohort was visualized in a oncoplot. Significant effects are highlighted in bold font and the numbers of cancer samples are shown above the plot. (B) Coexpression networks of genes encoding FGFR, FGF, or FGFBP whose expression levels correlated with Spearman's $\rho \geq 0.3$, visualized for the TCGA BLCA cohort with the Fruchterman-Reingold algorithm. Points represent genes, point shapes denote the protein product type and point colors the hub scores. Lines represent edges (ie, correlations with $\rho \geq 0.3$. The line widths correspond to ρ values. (C) Differential expression of genes encoding FGFR, FGF, or FGFR in consensus molecular classes of MIBC in terms of $\log_2$ mRNA levels between the LumP, LumU, stroma-rich, and Ba/Sq consensus molecular classes assessed via FDR-corrected one-way analysis of variance (ANOVA) with an η^2 effect-size statistic and a two-tailed post hoc t test. Differentially regulated genes were defined by $p_{ANOVA} < 0.05$, $\eta^2 \geq 0.14$, p_{FDR} (t test) < 0.05, and at least 1.25-fold regulation in a class in comparison to the LumP class. Z scores for $\log_2$ expression levels of differentially regulated genes shared by at least two cohorts are shown in a heat map for TCGA BLCA cancers. Significant effects are denoted with bold font and the numbers of samples are shown above the plot. (D) SHAP variable importance in the Elastic Net model of consensus molecular classes of MIBC with genes encoding FGFR, FGF, or FGFBP as explanatory factors. The contributions of the genes encoding FGFR, FGF, or FGFBP to prediction of LumP, LumU, stroma-rich, and Ba/Sq consensus molecular classes of MIBC according to the Elastic Net model were estimated using the SHAP algorithm (Shapley additive explanations). SHAP values for highly influential genes and observations are visualized in violin/swarm plots. Each point represents a single observation and point colors denote the minimum/maximum (min/max)-scaled $\log_2$-transformed gene expression. Mean absolute SHAP values as metrics of overall gene importance are presented in bar plots color coded for the association between SHAP values and gene expression (red = positive; blue = negative). (E) Sensitivity of DepMap urothelial cancer cell lines to pan-FGFR inhibitors. Resistance values in the PRISM (n = 17–23) drug screening experiment were expressed as AUC (area under the dose-response curve). Significant sensitivity was defined as AUC < 1, which indicates stronger growth inhibition than for the dimethylsulfoxide (DMSO) control. Doxorubicin was used as a positive cytotoxicity control. AUC values are depicted in violin plots; points represent single cell lines. Point colors denote *FGFR3* mutation status and shapes denote resistance versus sensitivity. The sensitivity cutoff is represented by the dashed line. (F) Sensitivity of *FGFR3* wild-type and mutant urothelial cancer cell lines to erdafitinib. Confluence of cell cultures of *FGFR1/2/3/4* wild-type (WT) cell lines (5637, RT-112, UM-UC-3) and *FGFR3* mutant cell lines (UM-UC-6, UM-UC-14) at 96 h after treatment with 0 (control), 1, 4, 7, and 10 μM erdafitinib. Points represent measurements for three independent biological replicates; data points obtained for the same replicate are connected with lines.

Please cite this article as: R. Pichler, Nils C.H. van Creij, L.S. Mertens et al., FGFR1/3 Signaling as an Achilles' Heel of Phenotypic Diversity in Urothelial Carcinoma, Eur Urol Oncol, https://doi.org/10.1016/j.euo.2025.07.005

Fig. 8). Analogously, a community of co-regulated genes encoding FGFR1 and its ligands and co-receptors was observed in UC cell lines (Supplementary Fig. 9). These data, together with the *FGFR3* mutation profiling, suggest that UC involves either ligand-dependent FGFR1 signaling or ligand-independent FGFR2/3 signaling.

Of the 45 transcripts and 49 FGFR-related gene signatures investigated, 22 mRNAs and 30 signatures were differentially expressed between consensus molecular subsets in at least two of the TCGA, IMvigor, and BCAN cohorts. *FGFR3*, *SDC1*, *TGFBR3*, *GPC3*, and *SDC4* were upregulated specifically in LumP cancers. Transcripts of *FGFR1* and FGFR1 ligands (*FGF7*, *FGF14*, *FGF10*, *FGF2*, *FGF9*, *FGF18*) and interaction partners (*DCN*, *HSPG2*, *SDC2*, *PTX3*), as well as most of the differentially regulated gene signatures, were enriched in the stroma-rich subtype suggesting ligand-dependent signaling. High expression of *FGF5*, *FGF11*, and genes coding for FGFBP, CD44, FGFBP1, GPC1 and TNFAIP6 was a hallmark of Ba/Sq cancers, indicative of ligand-dependent signaling via FGFR1 (Fig. 1C, Supplementary Figs. 10 and 11, and Supplementary Tables 7 and 8). Overexpression of *KL*, a gene encoding FGF19/FGF21/FGF23 co-receptors, was characteristic for luminal unstable (LumU) tumors. These data suggest distinct FGFR signaling mechanisms in LumP, stroma-rich, and Ba/Sq consensus molecular subsets (Fig. 2). These multifaceted FGFR signaling mechanisms are likely to be the reason for the high heterogeneity of in silico predicted responses to pan-FGFR inhibitor across the MIBC consensus classes and cancers with and without *FGFR3* mutations (Supplementary Figs. 12 and 13 and Supplementary Table 9).

Using two independent ML algorithms trained on transcript levels for 38 FGFR-, FGF-, and FGFBP-coding genes from the TCGA cohort, we reproduced the LumP, LumU, stroma-rich, and Ba/Sq consensus molecular subsets (IMvigor and BCAN validation cohorts: accuracy 0.72–0.84; AUC 0.92–0.97, Cohen's κ 0.59–0.77). In comparison to ML models using the full set of 818 MIBC consensus class–defining genes described by Kamoun et al [11], the FGFR/FGF/FGFBP gene models correctly predicted the LumP, stroma-rich, and Ba/Sq classes, but not the LumU class (Supplementary Figs. 14 and 15 and Supplementary Tables 10 and 11). This

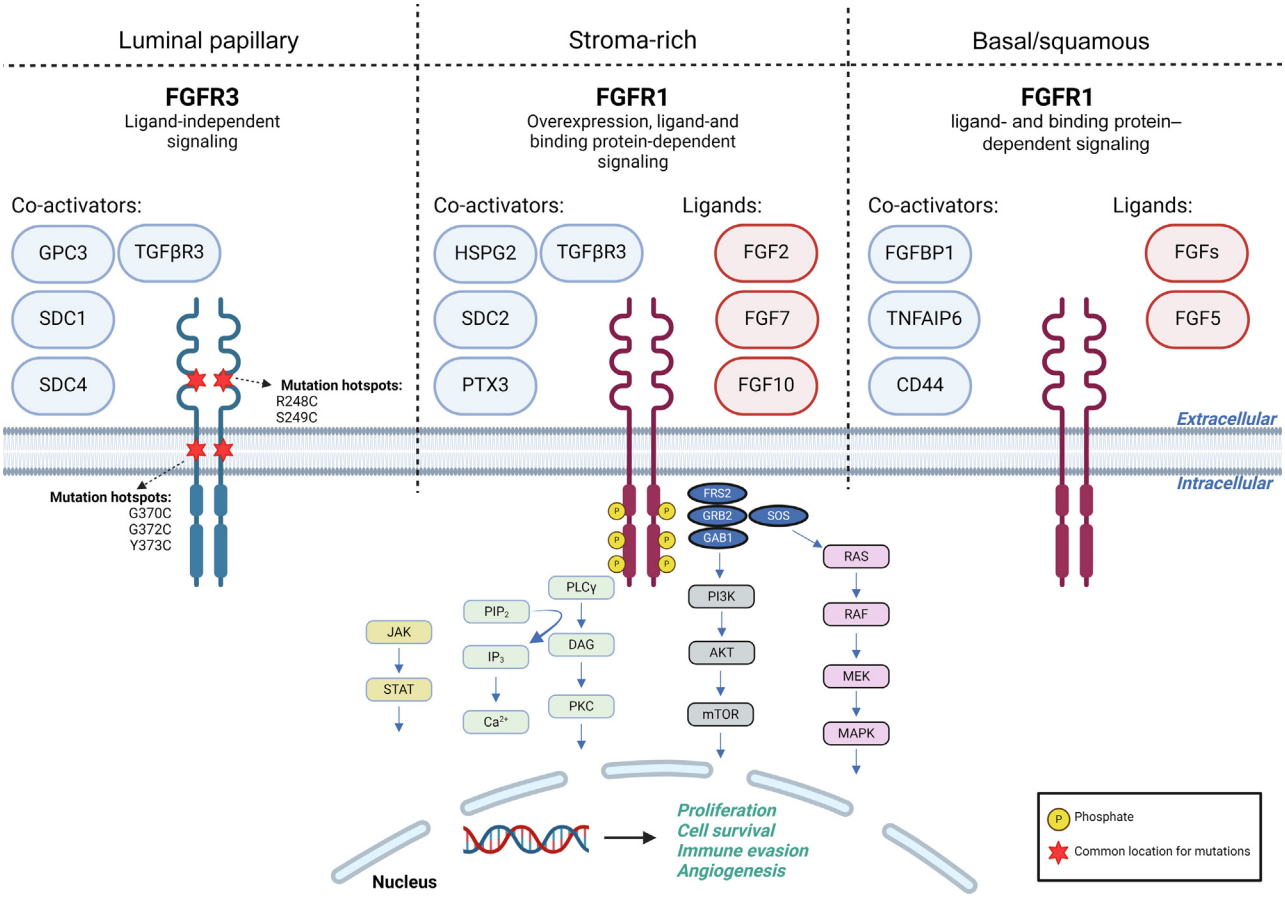

Fig. 2 – Distinct FGFR signaling activation according to molecular urothelial cancer subtype. Analysis of differential expression of genes encoding FGFR, FGF, and FGFBP genes was conducted for the consensus molecular subtypes [9] in the TCGA BLCA [5,6], IMvigor [7], and BCAN [8] cohorts. *FGFR3*, *SDC1*, *TGFBR3*, *GPC3*, and *SDC4* were upregulated specifically in luminal papillary cancers. FGFR3 mutations affecting the hinge regions of the protein product and overexpression of co-receptors and binding proteins TGFB3, SDC1, GPC3, and SDC4 may culminate in largely ligand-independent *FGFR3* signaling. Genes encoding FGFR protein and its ligands (*FGF7*, *FGF14*, *FGF10*, *FGF2*, *FGF9*, *FGF18*) and interaction partners (*DCN*, *HSPG2*, *SDC2*, *PTX3*) showed highest expression in the stroma-rich class. In stroma-rich cancers, this tightly coordinated overexpression of FGFR1 and its ligands (FGF2, FGF7, FGF9, FGF10, FGF14, FGF18) and interacting proteins (DCN, SDC1, HSPG2, ANOS1, and PTX3) may drive ligand-dependent FGFR1signaling. High expression of *FGF5*, *FGF11*, and genes encoding the binding proteins and FGF co-receptors *CD44*, *FGFBP1*, *GPC1*, and *TNFAIP6* was a hallmark of basal/squamous-like cancers. In basal/squamous tumors, overexpression of FGF5 and co-activators such as FGFBP1, CD44, and GPC1 triggers ligand-dependent signaling via FGFR1. Figure created with BioRender.com.

Please cite this article as: R. Pichler, Nils C.H. van Creij, L.S. Mertens et al., FGFR1/3 Signaling as an Achilles' Heel of Phenotypic Diversity in Urothelial Carcinoma, Eur Urol Oncol, https://doi.org/10.1016/j.euo.2025.07.005

supports findings from the differential expression analysis, which identified multiple FGFR/FGF/FGFBP-related markers of the LumP, stroma-rich and Ba/Sq classes, but not of the LumU class. The most influential genes for prediction of MIBC consensus classes identified by the Shapley additive explanations (SHAP) algorithm are outlined in Fig. 1D, Supplementary Figs. 16–19, and Supplementary Tables 12 and 13.

Finally, treatment of DepMap UC cell lines with pan-FGFR inhibitors in the GDSC1/2 and PRISM drug screens revealed that most UC cell lines were sensitive to pan-FGFR inhibitors, regardless of *FGFR3* mutation status (Fig. 1E and Supplementary Fig. 20). In vitro, erdafitinib reduced proliferation in *FGFR1–4* WT UC cell lines (UM-UC-3, 5637, and RT112) and the *FGFR3*-mutated UC cell line UM-UC-14^{S249C} in a dose-dependent manner. Interestingly, the *FGFR3*-mutated cell line UM-UC-6^{R248C} was resistant to erdafitinib (Fig. 1F and Supplementary Fig. 21). This, together with the in silico predictions of response to pan-FGFR inhibitors in the MIBC consensus classes and *FGFR3* WT/mutant cancers (Supplementary Figs. 12 and 13), highlights the potential benefit of FGFR inhibitor treatment beyond *FGFR2/3* alterations.

Limitations of our study include the incompleteness of clinical and multiomics data for the GENIE and MSK IMPACT cohorts, which precluded a comprehensive analysis of the transcriptome, gene signature, and drug response predictions. Furthermore, as our findings are based on statistical inference and modeling, we cannot establish causality, meaning that we cannot definitively demonstrate that FGFR signaling drives urothelial carcinogenesis in general. Lastly, the observational design, with a reliance on bioinformatics analyses, means that further clinical validation is needed.

In conclusion, differential gene expression in the consensus molecular MIBC subsets indicates distinct mechanisms of FGFR1/3 signaling activation. FGFR1/3 signaling may act as an Achilles' heel in UC that could justify FGFR-targeted therapy not only in LumP cancers and tumors with *FGFR2/3* alterations but also in other molecular subtypes. This fact is further supported by the widespread sensitivity of UC cell lines to erdafitinib in vitro regardless of *FGFR3* mutation status. FGFR signaling contributes substantially to UC phenotypes, as demonstrated by the accurate prediction of consensus molecular classes using only 38 FGF-related coding transcripts.

Author contributions: Renate Pichler had full access to all the data in the study and takes responsibility for the integrity of the data and the accuracy of the data analysis.

Study concept and design: Pichler, Pradére, Moschini, van Creij, Mertens, Subiela.
Acquisition of data: Tymoszuk, Pichler, van Creij, Günther, Subiela.
Analysis and interpretation of data: All authors.
Drafting of the manuscript: Pichler, van Creij, Pradére.
Critical revision of the manuscript for important intellectual content: All authors.
Statistical analysis, bioinformatics: Tymoszuk, Pichler.
Obtaining funding: None.
Administrative, technical, or material support: van Creij, Günther.
Supervision: Pradére, Li, Mertens, Moschini, Ormanns, Compérat.
Other (figure preparation): Pichler, van Creij.

Financial disclosures: Renate Pichler certifies that all conflicts of interest, including specific financial interests and relationships and affiliations relevant to the subject matter or materials discussed in the manuscript (eg, employment/affiliation, grants or funding, consultancies, honoraria, stock ownership or options, expert testimony, royalties, or patents filed, received, or pending), are the following: Renate Pichler reports institutional research funding from Bristol-Myers Squibb, Eisai, Ipsen, Merck, and Astellas Pharma; consulting fees from AstraZeneca, Eisai, Ipsen, Merck, MSD, Bristol-Myers Squibb, Astellas Pharma, and Johnson & Johnson; and a steering committee role for the MoonRISe-1 study (NCT06319820) sponsored by Johnson & Johnson. Laura S. Mertens reports institutional consulting fees from Johnson & Johnson and Merck. Gerald Klinglmair reports consulting fees and travel grants from Eisai, Ipsen, Astellas Pharma, Merck, and MSD. Roger Li reports a steering committee role for the MoonRISe-1 study (NCT06319820) sponsored by Johnson & Johnson; institutional research funding from Predicine, CG Oncology, and Valar Labs; and consulting fees from BMS, Merck, CG Oncology, Iconovir, ImmunityBio, Pfizer, Johnson & Johnson, AstraZeneca, and enGene. Henning Plage reports a sub-investigator role at Charité-Universitätsmedizin Berlin for the MoonRise-1 study (NCT06319820) sponsored by Johnson & Johnson. Benjamin Pradére reports a steering committee for the MoonRISe-1 study (NCT06319820) sponsored by Johnson & Johnson; consulting fees for advisory boards from Johnson & Johnson, BMS, Photocure, MSD, Pfizer, and Kranus Health; and speaker fees from Astellas, Pfizer, Johnson & Johnson, Ferring, MSD, and BMS. The remaining authors have nothing to disclose.

Acknowledgements: We sincerely thank Maxim Noeparast for providing the *FGFR3*-mutated urothelial cancer cell lines (UM-UC-6 and UM-UC-14) and Teresa Sellemond for her support with the cell culture models. We would also like to acknowledge the American Association for Cancer Research for financial and material support for the development of the AACR Project GENIE registry, and members of the consortium for their commitment to data sharing. The interpretations reported here are the responsibility of the study authors.

Appendix A. Supplementary material

Supplementary data to this article can be found online at https://doi.org/10.1016/j.euo.2025.07.005.

References

[1] Loriot Y, Matsubara N, Park SH, et al. Erdafitinib or chemotherapy in advanced or metastatic urothelial carcinoma. N Engl J Med 2023;389:1961–71.
[2] Catto JWF, Tran B, Rouprêt M, et al. Erdafitinib in BCG-treated high-risk non-muscle-invasive bladder cancer. Ann Oncol 2024;35:98–106.
[3] Siefker-Radtke AO, Lugowska I, Tupikowski K, et al. Clinical activity of vofatamab (V), an FGFR3 selective antibody in combination with pembrolizumab (P) in metastatic urothelial carcinoma (mUC), updated interim analysis of FIERCE-22. Ann Oncol 2019;30(Suppl 5):v365.
[4] Eisner JR, de Jong FC, Shibata Y, et al. Characterization of FGFR alterations and activation in patients with high-risk non-muscle-invasive bladder cancer. Clin Cancer Res 2024;30:5374–84.

[5] AACR Project GENIE Consortium. AACR Project GENIE: powering precision medicine through an international consortium. Cancer Discov 2017;7:818–31.
[6] Clinton TN, Chen Z, Wise H, et al. Genomic heterogeneity as a barrier to precision oncology in urothelial cancer. Cell Rep 2022;41:111859.
[7] Liu J, Lichtenberg T, Hoadley KA, et al. An integrated TCGA pan-cancer clinical data resource to drive high-quality survival outcome analytics. Cell 2018;173:400–416.e11.
[8] Robertson AG, Kim J, Al-Ahmadie H, et al. Comprehensive molecular characterization of muscle-invasive bladder cancer. Cell 2017;171:540–556.e25. https://doi.org/10.1016/j.cell.2017.09.007.
[9] Balar AV, Galsky MD, Rosenberg JE, et al. Atezolizumab as first-line treatment in cisplatin-ineligible patients with locally advanced and metastatic urothelial carcinoma: a single-arm, multicentre, phase 2 trial. Lancet 2017;389:67–76. https://doi.org/10.1016/S0140-6736(16)32455-2.
[10] Damrauer JS, Beckabir W, Klomp J, et al. Collaborative study from the bladder cancer advocacy network for the genomic analysis of metastatic urothelial cancer. Nat Commun 2022;13:6658.
[11] Kamoun A, de Reyniès A, Allory Y, et al. A consensus molecular classification of muscle-invasive bladder cancer. Eur Urol 2020;77:420–33. https://doi.org/10.1016/j.eururo.2019.09.006.
[12] Bonaventure J, Horne WC, Baron R. The localization of FGFR3 mutations causing thanatophoric dysplasia type I differentially affects phosphorylation, processing and ubiquitylation of the receptor. FEBS J 2007;274:3078–93. https://doi.org/10.1111/j.1742-4658.2007.05835.x.

Please cite this article as: R. Pichler, Nils C.H. van Creij, L.S. Mertens et al., FGFR1/3 Signaling as an Achilles' Heel of Phenotypic Diversity in Urothelial Carcinoma, Eur Urol Oncol, https://doi.org/10.1016/j.euo.2025.07.005